Electrochimica Acta 213 (2016) 752–760

Contents lists available at ScienceDirect

Electrochimica Acta

journal homepage: www.elsevier.com/locate/electacta

Fabrication of chiral mesoporous carbonaceous nanofibers and their electrochemical energy storage

Huayan Sun[a], Qing Wang[a], Hongbo Geng[a], Baozong Li[a], Yi Li[a,*], Qi-Hui Wu[b,*], Jingmin Fan[c], Yonggang Yang[a]

[a] Key Laboratory of Organic Synthesis of Jiangsu Province, College of Chemistry, Chemical Engineering and Materials Science, Soochow University, Suzhou 215123, PR China
[b] Department of Materials Chemistry, College of Chemical Engineering and Materials, Quanzhou Normal University, Quanzhou 362000, PR China
[c] Department of Chemistry, Xiamen University, Xiamen 361005, China

ARTICLE INFO

Article history:
Received 15 February 2016
Received in revised form 3 July 2016
Accepted 2 August 2016
Available online 2 August 2016

Keywords:
Mesoporous structure
Chiral carbon nanofibers
Supercapacitor
Lithium-ion storage

ABSTRACT

Chiral carbon-based nanomaterials possess many superior properties originated both from their nano-sized structure and their chirality. We presented a facile way to synthesize chiral mesoporous carbonaceous nanofibers (chiral MCNFs) through a supramolecular templating method, using a pair of chiral low-molecular-weight gelators as the templates, resorcinol, formaldehyde and tetraethyl orthosilicate as the precursors, respectively. Besides, the chiral MCNFs exhibited optical activity; the electrochemical measurements implied that they also showed good capacitance and lithium-ion storage performances.

1. Introduction

Ordered mesoporous carbon materials with controllable pore structure and size have attracted much attention because of their diverse applications in separation, catalysis, energy storage/conversion, and drug delivery [1–4]. Various methods have been developed for the synthesis of nanometer-sized mesoporous carbon-based materials. Remarkable progress has been achieved using a hard-template method, i.e. nanocasting approach [5–9]. Carbon precursors such as sucrose, furfuryl alcohol, ethylene gas, in situ polymerized phenol resin, and aromatic compounds were impregnated or deposited onto the mesopores of silica-based templates, after carbonization and removal of the used template material, mesoporous carbons were consequently fabricated. However, hard material templating is typically time-consuming and expensive to perform at a large quantity. Therefore, a soft-templating method based on supramolecular assemblies of surfactants and carbon precursors was designed and developed quickly in the past decade [10–14]. For example, by using Pluronic F127 and cetyltrimethyl ammonium bromide as the templates, resorcinol/formaldehyde (RF) resin derived mesoporous carbons have been successfully obtained, which presented preferable properties in adsorption, super-capacitors, and confined catalysis [10,11].

In recent years, helical carbon nanomaterials have aroused much interest for their potential applications in asymmetric catalysis [15], electromagnetic wave adsorption [16], single molecule sensor [17], and mechanical reinforcement [18]. To date, one-dimensional (1-D) helical carbon nanostructures, such as helical carbon nanoribbons, spring-like carbon nanowires, and helical carbon nanotubes have been reported [19,20]. They were commonly synthesized with chemical vapor deposition in the presence of catalysts. However, it is still hard to control the handedness of these 1-D carbon nanostructures. Recently, chiral carbonaceous nanostructures derived from chiral polymers such as polybissilsesquioxanes and polypyrroles have been reported [21–24]. Chiral polysilsesquioxanes were synthesized using self-assembly of chiral low-molecular-weight gelators (LMWGs) as templates and bissilsesquioxanes as precursors. After carbonization, chiral carbonaceous nanotubes, nanoribbons, and nanofibers with micropores within the walls were fabricated [21,22]. The micropores are mainly formed during the polycondensation of bissilsesquioxane, but which are largely disappeared after carbonization because of the thermal contraction [23]. Che et al. reported a one-step synthesis of enantiopure chiral carbonaceous nanotubes by carbonization of chiral polypyrrole nanotubes, which were templated by self-assembly of enantiopure chiral amphiphilic N-acylamino acid molecules and subsequent polymerization

* Corresponding authors.
E-mail addresses: liyi@suda.edu.cn (Y. Li), qhwu@qztc.edu.cn (Q.-H. Wu).

http://dx.doi.org/10.1016/j.electacta.2016.08.005
0013-4686/

of the bound pyrroles [24]. However, linear polymers might suffer great thermal deformation during pyrolysis. Compared with polysilsesquioxanes and polypyrroles, cross-linked phenolic resins possess higher yield of carbon conversion, more robust thermal stability, and better mechanical properties, which have been used as economic carbon precursors in synthesizing carbonaceous nanomaterials [14,25]. In the recent report, single-handed helical phenolic resin nanofibers have been successfully produced using chiral LMWG enantiomers as the templates, and they exhibited chirality at both the nano and the Ångstrom level [26]. The chiral resins can be used as precursors to prepare chiral carbons.

The aim of present work is to design and synthesize chiral MCNFs via a template duplication method and then study their electrochemical properties. First, single-handed helical resin-silica composite nanofibers were prepared in a one-pot reaction using a pair of LMWG enantiomers as the templates, resorcinol, formaldehyde and tertraethyl orthosilicate (TEOS) as the precursors. Then the resin-silica nanofibers were carbonized by annealing to form carbon-silica composite nanofibers. After removal of the silica with HF aqueous solution, chiral MCNFs were thus achieved, which, to our best knowledge, have not been reported previously. The chiral MCNFs were then characterized using field emission scanning electron microscopy (FE-SEM), transmission electron microscopy (TEM), Raman spectra, wide angle X-ray diffraction (WAXRD), ultraviolet-visible (UV) and circular dichroism (CD) spectra, and finally applied in supercapacitor and lithium-ion batteries (LIBs) as an electrode with high capacitance. The results indicated that the chirality has little influence on the lithium-ion storage of the chiral MCNFs, further, based on our experimental data the reason of the good electrochemical performance of the chiral MCNFs was proposed.

2. Experimental

2.1. Materials

LMWGs, *L*- and *D*-18Val11PyBr (their molecular structures are showed in Fig. 1), were synthesized according to the processes reported in the literature [22]. Resorcinol and formaldehyde (37–40 wt%) were purchased from Aldrich. Concentrated aqueous ammonium hydroxide (25–28 wt%) and TEOS were purchased from Sinopharm Chemical Reagent Co., Ltd.

2.2. Preparation of the single-handed helical resin-silica nanofibers

A typical synthesis route of the resin-silica nanofibers was as following: *L*-18Val11PyBr (or *D*-18Val11PyBr, 200 mg, 0.09 mmol) and resorcinol (180 mg, 1.6 mmol) were dissolved in deionized water (36 mL) and ethanol (4.0 mL) mixed solution at 40 °C under vigorous stirring. Then, concentrated ammonia aqueous solution (0.6 mL, 25–28 wt%), formaldehyde (0.23 mL, 37–40 wt%), and TEOS (0.8 mL, 3.6 mmol) were added into the solution in sequence. The reaction mixture was then stirred at 40 °C for 10 h, before heated upto 80 °C and stood in static for 24 h. The as-prepared product was collected by filtration and extracted with ethanol for 48 h, then dried in an oven at 50 °C for 24 h. The obtained samples are brown-reddish powders.

2.3. Preparation of the single-handed helical carbon-silica nanofibers

The obtained resin-silica sample was carbonized at 350 °C for 2.0 h and then 600 °C for 4.0 h with a heating rate of 1.0 °C per min in Ar atmosphere. After cooling to room temperature naturally, the carbon-silica samples were obtained.

2.4. Preparation of the chiral MCNFs

The carbon-silica samples were immersed in 10 wt% HF aqueous solution at room temperature for 24 h, followed by washing with deionized water for three times. The as-synthesized samples were then dried in vacuum at 40 °C overnight.

2.5. Characterization techniques

FE-SEM and the X-ray energy dispersive spectrometry (EDS) were performed using a Hitachi 4800 instrument at 3.0 kV and 15.0 kV, respectively. X-ray photoelectron spectroscopy (XPS, VG ESCALAB 220i-XL) was used to detect the surface composition and elemental oxidation states of the MCNFs. TEM images were obtained using an FEI TecnaiG220 at 200 kV. WAXRD patterns were collected with an X′ Pert-Pro MPD X-ray diffractometer using Cu Kα radiation (1.542 Å). Specific surface area and pore-size distribution were determined by the Brunauer-Emmett-Teller (BET) and Barrett-Joyner-Halon (BJH) methods using N_2 adsorption isotherm measured by a Micromeritics Tristar II 3020 instrument. Raman spectra were recorded using a Jobin Yvon Horiba HR 800 Labram confocal microprobe Raman system with Ar laser excitation (514.5 nm) and a power of 10 mW. The sizes of the silt and pinhole were 100 and 400 μm, respectively. UV and CD spectra were performed using an AVIV 410 spectrophotometer with a 1.0 nm bandwidth in a 0.1 cm cell at room temperature. The average time for a single scans is about 0.6 s. The CO_2 adsorption capacity was tested using an ASAP 2020 accelerated surface area and porosimetry instrument at room temperature. All electrochemical characterizations were completed on the CHI660c electrochemical workstation (Shanghai Chenhua Instruments Co.) at room temperature.

2.6. The electrochemical measurement

A three-electrode system in 6 mol L^{-1} aqueous electrolyte solution of KOH was used to characterize the electrochemical properties of the MCNFs. The Hg/HgO electrode and Pt plate were acted as the reference and counter electrodes, respectively. The test electrode was fabricated by loading 80 wt% carbon samples, 10 wt% acetylene black (AB) and 10 wt% polyvinylidene fluoride (PVDF) on the nickle foam under 10 MPa and dried at 100 °C for 24 h. Cyclic voltammetry (CV) curves were measured with a potential window of −1.0–0 V vs. Hg/HgO by changing the scans rates from 5 to 100 mv/s.

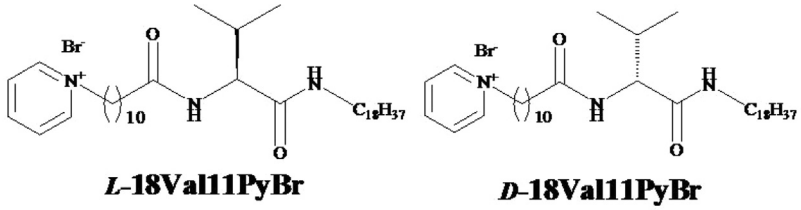

Fig. 1. Molecular structures of the LMWGs, *L*-18Val11PyBr, and *D*-18Val11PyBr.